

***greylock*: A Python Package for Measuring The Composition of Complex Datasets**

Phuc Nguyen, PhD^{a†}, Rohit Arora, PhD^{a†}, Elliot D. Hill, MSc^{a†}, Jasper Braun, PhD^{a†}, Alexandra Morgan^{a†}, Liza M. Quintana, MD^a, Gabrielle Mazzoni^a, Ghee Rye Lee, MSc^c, Rima Arnaout, MD^b, Ramy Arnaout, MD, DPhil^{a,1}

^aDepartment of Pathology, Beth Israel Deaconess Medical Center, Boston, MA 02215

^bDepartment of Medicine, University of California San Francisco, San Francisco, CA 94143

^cOhio State College of Medicine, The Ohio State University, Columbus, OH 43210

[†]These authors contributed equally to the manuscript.

¹To whom correspondence should be addressed at

Beth Israel Deaconess Medical Center
Department of Pathology
330 Brookline Avenue
Boston, MA 02215
rarnaout@bidmc.harvard.edu

Importance: *greylock* allows robust assessment of the composition of machine-learning and other large datasets using Python.

Keywords: data science, diversity, frequency, similarity, Shannon entropy, Simpson's index, metagenomics, immunomics, computational pathology, medical imaging, machine learning, Python.

Abstract

Machine-learning datasets are typically characterized by measuring their size and class balance. However, there exists a richer and potentially more useful set of measures, termed diversity measures, that incorporate elements' frequencies and between-element similarities. Although these have been available in the R and Julia programming languages for other applications, they have not been as readily available in Python, which is widely used for machine learning, and are not easily applied to machine-learning-sized datasets without special coding considerations. To address these issues, we developed *greylock*, a Python package that calculates diversity measures and is tailored to large datasets. *greylock* can calculate any of the frequency-sensitive measures of Hill's D-number framework, and going beyond Hill, their similarity-sensitive counterparts (Greylock is a mountain). *greylock* also outputs measures that compare datasets (β diversities). We first briefly review the D-number framework, illustrating how it incorporates elements' frequencies and between-element similarities. We then describe *greylock*'s key features and usage. We end with several examples—immunomics, metagenomics, computational pathology, and medical imaging—illustrating *greylock*'s applicability across a range of dataset types and fields.

Introduction

Assessing the size and quality of a dataset is an important part of machine learning in many fields (Table 1). How many unique elements are there, and how do they relate to each other? How do they cluster? Summary statistics provide initial answers and can form the basis for deeper questions. Historically, different statistics have featured more prominently in different areas of investigation. Examples include species richness in ecology, Shannon entropy in computer science, and Simpson's index in biology. In several fields, the practice is to bin elements before calculating statistics. For example, in metagenomics, sequences are usually binned into operational taxonomic units (OTUs); in immunomics, antibody and T-cell receptor (TCR) genes are often binned by lineage or antigen specificity. In machine learning, elements are binned by label to calculate class balance.

Frequency-sensitive diversity measures

It has long been known that the summary statistics above, among others, are related by how they account for differences in the relative frequency of repeated dataset elements [1]. For example, species richness, Shannon entropy, and Simpson's index, in that order, place an increasing emphasis on element frequency, essentially down-weighting elements that appear less frequently by having them contribute less to the statistic's final value. For example, in metagenomic datasets, species richness weights all OTUs the same regardless of how frequent they are, whereas in Simpson's index rare OTUs count less. In fact, these statistics are highly related to each other in that they are specific instances of a more general formula, known as Hill's diversity framework, in which the key parameter is the frequency down-weighting q (sometimes known as the "viewpoint parameter") [2]:

$$D_q = \left(\sum_{i=1}^n p_i^q \right)^{\frac{1}{1-q}} \quad \text{Eq. (1)}$$

(Note D_q also appears in the literature as qD .) In this equation, the dataset contains n unique elements and p_i is the frequency of the i^{th} unique element in the dataset. In the limit of $q = 1$, Eq. (1) approaches $\exp(-\sum_i p_i \ln p_i)$, which is the exponential of the Shannon entropy [3]. The only substantive difference between species richness, Shannon entropy, Simpson's index, and many other summary statistics is in the value of q : $q = 0$ for species richness (all elements count the same), $q = 1$ for Shannon entropy (some down-weighting of rare elements), $q = 2$ for Simpson's index (more down-weighting), and so on up to $q = \infty$ for the Berger-Parker index (maximum down-weighting) [4], for which the frequency of only the most common element matters.

Effective numbers

The D numbers of Hill's framework yield the so-called *effective number* forms of Shannon entropy, Simpson's index, and so on. These give the effective number of elements in a dataset, for a given weight q . For example, if two immunology datasets contain the same number of unique antibody sequences but the first dataset has a sequence that accounts for 90% of all sequences in the dataset (as can happen in leukemia), the first dataset will have a lower effective number of sequences for $q > 0$. Likely the effective number of species will be not much more than 1, since to a good approximation—"effectively"—the dataset consists of just the one dominant sequence. Fig. 1 illustrates this concept in a discipline-agnostic manner. The commonly used forms of the above statistics are simple mathematical transformations of the effective-number forms: for example, Shannon entropy is the logarithm of D_1 , while Simpson's index is the reciprocal of D_2 . For the investigator, the advantages of using effective numbers are, first, effective numbers all have the same units, allowing them to be easily compared; and second, they behave nicely as datasets are combined or split apart. Non-effective-number forms generally lack these properties [5].

The effective number of elements in a dataset (at some q) is a natural measure of dataset size, complexity, or diversity [6]. Because this number can also be thought of as a measure of how diverse the dataset is, the D numbers are also known as diversity measures (or diversity indices): "diversities of order q ." More specifically, when $q > 0$, they are *frequency-sensitive diversity measures*. Within- and between-dataset measures are known as alpha and beta diversity, respectively.

Similarity-sensitive diversity measures

When grouping elements is called for, such as for OTUs and antibody/TCR clusters, a similar approach to Eq. 1 can be used, provided that the similarity between each pair of elements is accounted for. Such accounting is possible through an extension of Hill's framework that outputs similarity-sensitive versions of the D numbers, shown by Leinster and Cobbold [2]. For each pair of unique elements in the dataset, the investigator supplies a *similarity* between 0 and 1, with 0 meaning the two elements are completely different and 1 meaning they are identical. Similarities are provided as entries in a table or matrix. This is called the similarity matrix, Z , a square matrix of dimension n (where again n is the number of unique elements). In the context of network science or graph theory, Z can be thought of as an adjacency matrix with self-edges added to make the diagonal entries all equal to 1.

In practice, especially for large datasets, Z is populated computationally according to an investigator-provided formula or rule. Binning can be understood as a special case where the cell Z_{ij} that corresponds to the similarity between elements i and j is set to 1 if i and j are in the same bin and set to 0 otherwise. For example, for OTUs the similarity is set to 1 if two 16S rRNAs have greater than a threshold-level of sequence identity (e.g. $\geq 95\%$ or $\geq 99\%$), placing them in the same OTU, and 0 otherwise (but see below for a continuous alternative). However, in general similarities Z_{ij} can take any value between 0 and 1. They can be fractional (0.9, 0.327..., etc.) or even asymmetric, with element i more similar to element j than element j to element i ; the decision is up to the investigator [7]. Some examples of similarity measures include the well-known structural similarity index measure (SSIM) for images [8], [9] and relative dissociation constants for proteins and other molecules [10].

Mathematically, incorporating Z yields the following equation:

$$D_q^Z = \left(\sum_{i=1}^n p_i (Z\mathbf{p}_i)^{q-1} \right)^{1/(1-q)} \quad \text{Eq. (2)}$$

Here, $Z\mathbf{p}_i = \sum_j Z_{ij}p_j$ is the “ordinariness” of the i^{th} unique element, i.e. the cumulative similarity of the i^{th} unique element to all the other elements of the dataset [2]. The Z in D_q^Z designates these measures as being *similarity-sensitive* D numbers; the presence of q in Eq. 2 means that these similarity-sensitive diversity measures are also frequency sensitive, like the D_q numbers of Eq. 1. Fig. 2 provides a discipline-agnostic illustration. Note that interpreting Z as an adjacency matrix, Eq. 2 can be used to provide measures of network complexity in e.g. social networks or gene-interaction networks (Table 1).

Advantages of similarity-sensitive measures

Similarity-sensitive D numbers have several advantages over their similarity-insensitive counterparts. First, similarity-sensitive D numbers align better with an intuitive sense of what “diversity” and “complexity” should mean [6], [7]. For example, given two otherwise identical 16S rRNA microbiome datasets, the dataset that represents the greater number of taxa is intuitively more diverse. Consistent with this intuition, it will have the higher D_q^Z (see Metagenomics below). In contrast, the two datasets will have identical D_q , thus, the similarity-insensitive D_q measures will miss the main difference between these datasets.

Second, D_q^Z measures capture the effects of grouping without the need to choose a binning threshold (e.g. 95% vs. 99% sequence identity for OTUs [11], [12], or a radius of 1 vs. 2 vs. 3 nucleotide differences for clone membership [13]). There is also no need to place an element

exclusively into a single group: multiple and/or fuzzy group membership is inherently allowed. This flexibility is especially useful for image datasets, where D_q^Z simultaneously captures the number of classes as well as the diversity within and between classes [14].

Third, D_q^Z measures provide rich mechanisms for exploring higher- and lower-level dataset structure, including a well-developed framework for partitioning within- (alpha) vs. between- (beta) dataset diversity. It also offers a ready method for investigating substructure using the ordinariness, $Z\mathbf{p}_i$. For example, to measure how “Enterobacterales-like” a given 16S rRNA dataset is, if the ordinariness to a given Enterobacterales sequence (or set of sequences) is high, the dataset is very Enterobacterales-like. This method could be useful for quantitative definitions and assessments of enterotypes (see Results).

We stress that the usefulness of these diversity indices extends well beyond any one field. Table 1 lists several possible applications of frequency- and similarity-sensitive diversity measurements in different areas, from engineering to the natural and social sciences.

Representativeness as a measure of overlap between datasets

The framework in Eq. 2 extends naturally to measures of between-dataset diversity, also known as beta diversity [15]. Given a pair of datasets A and B , $\bar{\beta}_A$ describes how distinctive dataset A is, with a value of 1 meaning indistinguishable and 2 meaning completely distinct. (We write out “beta” when referring to beta diversity so as not to confuse it with $\bar{\beta}$; unfortunately dual-use of this Greek letter is a convention in the literature.) Alternatively, we can use the *representativeness*, which is the inverse of distinctiveness and which is a more straightforward measure of overlap: representativeness of 1 means the dataset A is completely representative of the pair, whereas a zero-overlap dataset has 0.5 representativeness, because it is precisely half of the pair. (The minimum value is $1/N$ for N datasets.) Mathematically, representativeness is written $\bar{\rho}$ and is the reciprocal of $\bar{\beta}$. We can also use (as an overlap measure) the diversity index R , which is the average of the representativenesses of the two datasets and which is known as the *redundancy* of the pair. Note, the original formulation of the framework [2] uses the terms “community” and “metacommunity” in place of “dataset” and “pair” or larger grouping, reflecting its roots in ecology; for this reason, we use these terms in the classes and methods of the *greylock* package.

Prior work and present contribution

The need for summary statistics that address the above-described issues has been well

documented in metagenomics and immunology [10]–[12], [16]. Other mathematical frameworks similar to the one in Eq. 2 have been proposed [17]. Packages for calculating frequency- and similarity-sensitive α and β diversities in effective-number form exist for the R and Julia programming languages [18], [19], but not to our knowledge for Python, which is more widely used, especially in machine learning.

Of note, large datasets present a special challenge for measuring similarity-sensitive diversity: because Eqs. 1-2 require calculating the similarity between each pair of the n unique species in the dataset, and because these pairwise similarities are usually inputted as elements of an $n \times n$ matrix, direct implementations risk running out of computer memory when n is large. For example, assuming standard 8-byte floating point precision, a single dataset of a million unique elements would require 8TB of memory. Immunomes, metagenomes, and imaging datasets routinely contain tens or hundreds of thousands of unique elements [20], as do transcriptomes, cell atlases, and other complex datasets. Moreover, a single study can involve tens to hundreds of such datasets (e.g., one per sample/volunteer/patient) and thereby many millions of unique elements in all. The R package *rdiversity* and the Julia package *Diversity* both require a similarity matrix stored in memory, but for the applications above such matrices are likely to be too large to store in working memory and may even be too large to write to disk. In contrast, *greylock* implements on-the-fly row-by-row calculations, to better handle such cases. The Python package *cdiversity* calculates Hill-number diversity but without similarity for immune repertoires [21], [22].

In addition to the standard diversity indices in the β family, we introduce two new quantities, $\hat{\rho}$ and $\hat{\beta}$ (“ ρ -hat” and “ β -hat”), which are normalized versions of $\bar{\rho}$ and $\bar{\beta}$. The reason is that $\bar{\rho}$ itself can be a very large number if there are a large number of datasets in the study (i.e., a large number of subcommunities in the metacommunity). So, roughly speaking we can divide $\bar{\rho}$ by the number of subcommunities to obtain a measure of redundancy that usually ranges from 0 to 1. (Note the upper bound may not be respected in extreme or pathologic cases, but these will be the exception.)

Results

Python package overview and main features

greylock was developed to simplify the calculation of frequency- and similarity-sensitive diversity measures for Python users. It has the ability to calculate all frequency- and similarity-sensitive

diversity measures presented in Reeve et al.'s work [15], as well as their similarity-insensitive counterparts. It offers command-line execution as a Python module for similarity-sensitive diversity calculations using a similarity matrix stored on disk and also provides a convenient interface when imported as a Python package. Installation and usage instructions can be found in the Supplementary Material.

Applications

We now illustrate some practical applications of *greylock* using sample datasets from the fields of immunomics, metagenomics, medical imaging, and computational pathology, as examples of the many types of dataset to which this package can be usefully applied. Jupyter notebooks with these examples are available in the Supplementary Material and via the *greylock* GitHub repository.

Immunomics

Antibody (IG) and T-cell receptor (TR) repertoires are famously diverse, with tens of thousands of different IG and TR gene sequences in every milliliter of human blood [16], [20], [23]–[25]. The frequency of a given sequence rises with exposure to antigens as cells divide, forming clones of identical or similar sequences, and falls to baseline over time as cells die. As a result, measures that are both frequency-sensitive and similarity-sensitive are useful for describing the state of the adaptive immune system [10], [16], [26].

To illustrate, we revisit a set of 30 IG heavy-chain (IGH) repertoires from 15 subjects taken before and after influenza vaccination [27], each subsampled to a same-sized 100,000-sequence subset [10]. Vaccination is associated with an increase in the number of sequences— D_0 , which is similarity insensitive—interpreted as vaccination leading to new sequences [27], a finding confirmed in a recent re-analysis of the data [10] that corrected for sampling bias (using the *recon* package [16]) (Fig. 3a). We can use *greylock* to measure the alpha diversity for each before-and-after pair using the similarity-sensitive diversity measure D_0^Z , using binding similarity as previously described to construct the similarity matrix [10]. Unlike D_0 , which generally rises as antigen-responsive cells divide and accumulate mutations, D_0^Z falls in 12 of the 15 subjects (Fig. 3b). The combination of these two trends tells us that new sequences that are seen following vaccination are likely related, consistent with expansion of pre-existing clones. The three exceptions suggest something different is happening immunologically in these subjects, perhaps new immune responses or fewer mutations.

Metagenomics

Measuring diversity is also of interest in metagenomics, where microbiomes from e.g. stool or soil samples are high-throughput sequenced to determine the number and frequency of species present. For practical reasons, often the sequenced material is not a complete genomes but telltale genes, such as 16S rRNA sequences, or fragments of such genes [28].

This task is challenging for three reasons. First, the concept of “species” is not as well defined for bacteria as it is for more complex organisms. Second, the similarity of a pair of species, measured in terms of phylogeny or sequence identity, can differ substantially from pair to pair, such that a pair of organisms with a given degree of sequence identity might be classified as the same species in one genus but as distinct species—or even distinct genera—in another. Third, many recovered sequences are difficult to map uniquely to known species. (Tools such as Unifrac that characterize the similarity between microbiomes according to the proportion of shared lineages still require confidence in lineage assignment [29].) These three challenges are in addition to the general challenge faced in measuring the diversity of complex populations: assuring that the diversity of the sample is an accurate representation of the diversity of the population from which the sample was drawn [16].

To address these three challenges, a common first step in measuring microbiome diversity has been to bin sequences into OTUs based on a set threshold level of sequence similarity, e.g. 95% or 97%. Unfortunately, binning is not without its own challenges [11], [12]. First is the problem of “adverse triplets” [12]: sequences i , j , and k for which the similarity between i and j is above the threshold, the similarity between j and k is also above the threshold, but the similarity between i and k is below the threshold. Binning all three into the same OTU because i - j and j - k are above the threshold results in the OTU containing i and k even though their similarity is below the threshold. A second challenge is determining what the appropriate threshold should be [11], [12]. These are general problems with binning or other forms of unique assignment. I.e. they are not specific to metagenomics: they are a necessary consequence of discretization of continuous or near-continuous variables, such as sequence similarity, into discrete bins.

Similarity-sensitive measures offer an alternative way to measure the diversity of microbiomes. We used *greylock* to illustrate using synthetic/*in silico* microbiome samples reminiscent of enterotypes in human gut microbiomes [30], [31]. An enterotype is a microbiome that exhibits a certain compositional pattern, e.g. enrichment in bacteria of the genus *Bacteroides* [30], [32]–[34]. Consider the two samples in Fig. 4. Both have clusters of similar sequences; Sample 1 has

five highly distinctive clusters (Fig. 4a) while Sample 2 has 10 clusters that are all fairly similar to each other (Fig. 4b). Similarity can be accounted for in two ways: by binning and then using similarity-insensitive measures or by *not* binning and instead using similarity-sensitive diversity measures.

These yield different results. Binning sequences yields diversity values that depend on the choice of binning threshold but generally show Sample 2 as having higher diversity, reflecting the larger number of clusters (Fig. 4c, d). In contrast, similarity-sensitive measures show Sample 1 as having higher diversity, reflecting the larger range that the sequences in Sample 2 span (Fig. 4e). Specifically, D_0^Z is a little over 5.4 in Sample 1, reflecting the five distinct clusters plus their (limited) intra-cluster diversity, whereas it is 3.6 in Sample 2, reflecting that the 10 clusters are themselves highly related (“effectively” having the same diversity as a sample with 3.6 completely distinct sequences).

The *greylock* package is also useful for investigating population structure across different samples (subcommunities), for example to identify correlates of disease [35]. One way to do so is by defining the similarity s_{ij} between each pair of unique sequences i and j , treating each pair of samples as its own metacommunity, and then using s_{ij} to calculate how well each sample k represents the pair. This can be done either using the quantity, $\bar{\rho}_k$, which is the representativeness of sample k , or \bar{R} , which is the average representativeness over both samples in the pair. $\bar{\rho}_k$ generally differs for each sample in the pair, reflecting asymmetries in the overlap between them; in contrast \bar{R} is always symmetric, and so should be thought of as an attribute of the pair, not of the constituent samples. Note $\bar{\rho}_k$ can be calculated at any q ; in this example we omit the q subscript for readability and use $q = 0$ unless otherwise specified. *greylock* readily calculates $\bar{\rho}_k$ and \bar{R} for any q . Once calculated, one can use these values to investigate population structure by clustering on the resulting matrix (Fig. 5).

For example, consider the nine synthetic samples in Fig. 5a. Using the same s_{ij} as in the previous example, clustering by either $\bar{\rho}_k$ (Fig. 5b) or \bar{R} (Fig. 5c) clearly shows these samples cluster into three enterotypes. Alternatively, one could instead use the OTU approach: account for similarity by choosing a sequence-similarity threshold τ , bin according to that threshold, and then use *greylock* without s_{ij} to calculate and cluster on $\bar{\rho}_k$. However, OTU results are highly sensitive to the choice of threshold (Fig. 5d-e). The block structure is discernable only in the dendrogram in Fig. 5d, whereas there is no obvious clustering apparent in Fig. 5e. Note that both approaches require a choice about how similar two sequences are: in the former case via s_{ij} and in the latter via τ . (Recall that choosing $s_{ij} = 1$ for sequences whose similarity is $\leq \tau$ and $s_{ij} = 0$ otherwise makes the latter a special case of the former, except without the problem of

adverse triplets.) The choice of s_{ij} will depend on the context (sequence similarity, phylogenetic similarity, functional similarity, etc.).

Medical Imaging

Medical imaging is an active area of interest in machine learning (ML). Examples include view- and disease-classification tasks on X-rays, magnetic-resonance imaging (MRI) and positron-emission tomography (PET) scans, and ultrasounds (the most widely used and cost-effective modality for internal imaging). Training ML models on these and other types of medical images usually requires large, class-balanced medical-imaging datasets [9]. This section illustrates use of the *greylock* package to characterize such datasets, using an echocardiogram dataset as an example [36].

The dataset consists of 136 cardiac ultrasound images (echocardiograms) labeled for five classes according to which of five views of the heart they show (A4C, A5C, 3VV, ABDO, and 3VT), selected for ease of illustration (Fig. 6). Unlike the previously discussed examples, in medical-imaging datasets each element generally appears only once, so all the images occur with the same frequency ($1/n$, where n is the total number of images in the dataset, i.e. the dataset size). As a result, image frequency is generally not very informative in characterizing the dataset. However, similarity can be, as we show.

We suppose that only half the images in this dataset are already labeled. We want a sense of what might be gained through the effort of labeling the other half. We know the size of our labeled dataset would double. Assuming that ML benefits from datasets that are not only large but diverse, how much actual diversity would we add? We can answer this question by asking how well each half reflects the composition of the full dataset. The preceding section illustrated the utility of $\bar{\rho}_k$ for this purpose. Here we will use a related measure introduced in the *greylock* package: $\hat{\rho}_k$ (“rho-hat”), defined as $\hat{\rho}_k = (\rho_k - 1)/(N - 1)$, where N is the number of subsets. $\hat{\rho}_k$ has the convenient property of ranging from 0 to 1 (except for extreme/pathological cases), which may be more interpretable than the alternatives. A subset k that is maximally distinctive relative to the full dataset will have $\hat{\rho}_k = 0$ while a subset that is maximally redundant will have $\hat{\rho}_k = 1$.

To illustrate the utility of $\hat{\rho}_k$, consider two different splits of the dataset, both even. Call the subsets that result from the first split A and B and the subsets from the second split C and D . In each case, we assume one of the halves is already labeled. For each split, we calculate $\hat{\rho}_k$ for each subset relative to the whole dataset, using an RMSE-based similarity (Fig. 6). We find that

$\hat{\rho}_A$ and $\hat{\rho}_B$ are both ~ 1 : both are as diverse as the overall dataset, even though they are each only half the size (Fig. 7). If either of these subsets is labeled, labeling the other adds very little diversity. In contrast, $\hat{\rho}_C$ and $\hat{\rho}_D$ are only 0.6-0.7: labeling the other half would increase diversity substantially.

Currently, the most commonly used heuristics for dataset composition are size and class balance (measured as e.g. the Shannon entropy of the label frequencies). That A , B , C , and D are the same size ($n = 68$ images) and have essentially the same class balance (1.27-1.28, vs. 1.28 for the full dataset) yet differ markedly in $\hat{\rho}_k$ demonstrates that this new measure can capture information about datasets that size and class balance alone do not. This ability may be useful in other datasets [37]–[39] and as a new way to quantify the value of different forms of data augmentation [40].

Computational pathology

Finally, we illustrate *greylock* on a much larger ML imaging dataset of histological slide images. We use 89,996 training-set images of haematoxylin/eosin (H&E)-stained colon tissue sections from the PathMNIST subset of the MedMNIST database [41]. These are 28x28-pixel images of patches of 1,000-fold-magnified microscopic fields from each slide that can contain any of the many structures found in healthy and diseased colon tissue, including fat, muscle, and blood vessels as well as colonic epithelium (Fig. 8a).

Continuing the theme of the previous section, we use *greylock* to ask how much of the dataset’s diversity is captured by randomly chosen smaller subsets. Specifically, we created subsets of increasing size and measure $\hat{\rho}_k$ on each of them, relative to the entire dataset. Because this dataset is much larger than the previous examples, *greylock*’s on-the-fly similarity matrix option is used, as opposed to pre-calculating the similarity matrix and then loading it from memory as in the previous sections. This is done by passing *greylock* a function for calculating the similarities between pairs of images s_{ij} . For this example, the function was designed to approximate human pathologists’ determination of pairwise similarity between images (Fig. 8b), reaching agreement of $R^2 = 0.48$ with each of two experts (on 100 image pairs) vs. an inter-expert R^2 of 0.57. We find that even small subsets capture a substantial fraction of the diversity of the full dataset: for example, subsets of 512 randomly chosen images—less than 1% of the full dataset—capture $\geq 95\%$ of the diversity ($p = 0.99$) (Fig. 8c).

Discussion

Frequency- and especially similarity-sensitive diversity measures are useful for characterizing complex datasets. Here we have introduced and described *greylock*, a Python package for calculating them, and demonstrated various applications using examples in immunomics, metagenomics, medical imaging, and computational pathology. *greylock* is available via PyPI and installed using the standard package manager (pip) for ease of use.

The recasting of simple counting (richness), Shannon entropy, Simpson's index, and other measures as special cases of a single framework will be new to some investigators but has two advantages. First, it renders these otherwise disparate measures in the same unit—effective number of unique elements—allowing them to be directly compared. And second, it demonstrates that the only difference among them is in how they weight elements' frequencies. However, it recasts investigators' decision of which measure(s) to use as a decision of how much weighting is appropriate for a given investigation—i.e., which q to use. One can avoid this choice by essentially using all of them (e.g. Fig. 4c-e). This option captures much more information and avoids the possibility of inadvertently cherry-picking a measure that might miss some important feature of the dataset at hand. *greylock* outputs results for $q = 0$ to ∞ .

In contrast, a choice that cannot be avoided is the choice of similarity measure s_{ij} when calculating similarity-sensitive measures. The same set of elements may be similar in different ways: physiologically, genetically, functionally, constructively, etc. This includes settings that can in principle be quite complex, for example when the similarity between a pair of elements is a function of elements' frequencies, leading to complicated expressions for s_{ij} . Because calculation of similarity-sensitive diversity measures (D_q^Z) requires s_{ij} for all pairs of n unique elements in the dataset, the time required calculating similarity-sensitive measures scales as $\mathcal{O}(n^2)$. *greylock* is implemented with parallelization to make use of multicore processors, allowing datasets of 10^5 - 10^6 elements in under a day on a standard workstation. However, there is opportunity on this rate-limiting step for algorithmic improvement.

The examples presented highlight the complementarity of similarity-insensitive and similarity-sensitive measures (immunomics), the utility of the continuous nature of similarity-sensitive measures (metagenomics), and the value of similarity-sensitive measures for dataset assembly and assessing dataset quality (machine learning). In the latter context, diversity may prove useful for dataset curation, the need for which has been recognized as a national priority [42]. Given the diversity of these examples, we expect other fields (Table 1) will also benefit from the D_q^Z -number Hill framework as brought to Python via the *greylock* package.

Methods

Python package. The package was developed and described as in the main text.

Immunomes. Immunomes were obtained and processed, and similarity was calculated, as previously described [10].

Metagenomes. To construct each synthetic dataset, gaussian sampling to single-decimal-place precision was performed around each of a set of mean values between 0 and 100 to create a gaussian distribution of sequence frequencies around each mean. In Fig. 4, the same number of sequences was sampled around each mean. In Fig. 5, we sampled four times as many sequences around one of the means, which was selected as the dominant taxonomic unit defining the enterotype (a different dominant mean for each enterotype).

Medical imaging. Images were selected at random from the dataset introduced and processed as previously described [36].

Computational pathology. The 89,996-image PathMNIST training set is a component of MedMNIST, as previously described [41].

Preprocessing. The dataset was filtered to keep only the 82,698 images that contained specimen (removing e.g. nearly-all-black or -blue images, which are likely off the slide or pictures of marker on the slide). Regions surrounding tissue or corresponding to tears in the tissue were thresholded to white. Hue and lightness were obtained as the H and L channels from the standard HLS colorspace using the Python image library Pillow (v8.2.0).

Similarity s_{ij} between each pair of images i and j was determined as the minimum of the similarities of four component features: hue, lightness, texture (e.g. sheets of nuclei), and structure (e.g. colonic crypts), as detailed below. This expert-feature engineering approach was used as it provided rapid proof of principle based on expert knowledge with a minimal set of human-expert examples (as opposed to a more involved/more data-hungry machine-learning approach).

Hue component. The hue component was the overlap between hue histograms.

Lightness component. The lightness component was the overlap between lightness histograms between 0.2 and 1.0, binned into 28 bins.

Texture component. The texture component was a function of the similarity of mottledness (e.g. nuclei, sheets of cells) and stripedness (e.g. muscle fibers). The mottledness m_i of an image i was defined as the mean over all pixels of the maximum lightness difference $\delta_{\max i}$ between a pixel and each of its eight nearest neighbors (normalized by the range of observed values, which happens to be 0.39): $m_i = \bar{\delta}_{\max i} / 0.39$, (where the bar indicates averaging). The mottledness similarity m_{ij} between images i and j was then defined as $m_{ij} = 0.1$ if $m_i < 0.5$ and $m_j > 0.5$, and $m_{ij} = 1 - |m_i - m_j|$ otherwise. Stripedness of an image i was calculated in four directions: horizontal, vertical, and the two diagonals ($\sigma_{\uparrow i}$, $\sigma_{\rightarrow i}$, $\sigma_{\nwarrow i}$, $\sigma_{\nearrow i}$, respectively). In each case, it was defined as one minus the mean over all pixels of the sum of the differences δ_i between a pixel i and its nearest neighbor in each direction (e.g., for horizontal stripedness, its neighbors to the left and right) times the sum $\delta_{\perp i}$ of the neighbors in the perpendicular direction (for horizontal stripedness, its neighbors above and below), again normalized by the range of observed values: $\sigma_{_i} = (1 - \bar{\delta}_i) \bar{\delta}_{\perp i} / c_{_}$ for each direction (where $_$ is replaced by \uparrow , \rightarrow , \nwarrow , or \nearrow and the normalization constants were $c_{\uparrow} = 0.229$, $c_{\rightarrow} = 0.240$, and $c_{\nwarrow} = c_{\nearrow} = 0.226$). The stripedness for the image as a whole, σ_i , was defined as the max of $\sigma_{\uparrow i}$, $\sigma_{\rightarrow i}$, $\sigma_{\nwarrow i}$, and $\sigma_{\nearrow i}$. The stripedness similarity σ_{ij} was defined similarly to mottledness similarity: $\sigma_{ij} = 0.1$ if $\sigma_i < 0.5$ and $\sigma_j > 0.5$, and $\sigma_{ij} = 1 - |\sigma_i - \sigma_j|$ otherwise. The texture similarity was then defined as $t_{ij} = \min(m_{ij}, \sigma_{ij})$.

Structure component. A median filter was applied to each image to ignore outlier pixels. The structure component was then defined as the minimum of two subcomponents: similarity of structure size S_{ij} and similarity of number of “holes” in the image H_{ij} .

S_{ij} was determined as follows. If the resulting image had nearly uniform lightness (lightness range < 0.5), S_{ij} was ignored (because meaningful structures could not be easily extracted). For remaining images, structure size was determined by segmenting to find the largest patch P_i around the darkest pixel in each image i . Thereafter, the following conditional logic was applied. If the largest structure in both images in the pair was < 30 pixels, S_{ij} was again ignored (structures were likely noise). Otherwise, the difference in lightness of the darkest pixel of each image was calculated (Δ). If Δ was > 0.2 times the lightness range of image i and if P_i was < 30 pixels, S_{ij} was again ignored; if P_i was ≥ 30 pixels, $S_{ij} = 0$. If instead Δ was ≤ 0.2 times the lightness range of image, and if in addition over half the pixels in each image had lightness > 0.8 (e.g. indicating fat), $S_{ij} = 0.9$. Otherwise, if over 60 percent of the pixels in one of the two images had lightness > 0.8 (meaning one was very light and the other very dark), $S_{ij} = 0.1$. Otherwise, S_{ij} was set to be the size ratio of the smaller to the larger patch.

H_{ij} was determined as follows. For each image i , the mask used to find P_i was examined to count the number of light patches. (Patches that were only a single pixel in size were

considered noise and ignored.) Each light patch was considered a hole. There was always at least 1 hole. H_{ij} was defined as the ratio of the smaller to the larger number of holes for the pair of images. Structure similarity was defined as $\min(S_{ij}, H_{ij})$.

Comparison to human experts. 100 image pairs were selected representing the range of similarities according to the above similarity function (from 0 to 1) and presented independently to two practicing pathologists. These domain experts were instructed to assign the similarity between the two images, without further instruction, on a 1 to 10 scale. R^2 was calculated between their similarity scores as a measure of inter-expert agreement, and separately between each of their scores and s_{ij} .

Funding

This work was supported by the NIH (R01AI148747-01), the Gordon and Betty Moore Foundation (RA), and the Massachusetts Life Sciences Center.

Tables and Figures

Table 1: Datasets amenable to frequency- and similarity-sensitive Diversity measurements

Engineering/ Industry	Medicine/ Health	Biology/ Ecology	Physical Sciences	Human Activities
Other ML datasets	Medical imaging datasets	Immunomes	Astronomical objects	Populations
ML models/ ensembles	Diseases	Microbiomes	Geography and terrain	Societies
Machine parts	Patient cohorts	Viromes	Chemical compounds	Political organizations
Supply chains	Medications	Transcriptomes	Minerals	Boards of directors
Industries	Foods	Sequencing libraries		Artwork
Investment portfolios		Ecosystems/ biomes		Classrooms
		Gene-interaction networks		Admission/hiring/ promotion/review committees
				Social networks
				Sports teams and leagues

Table 2: Datasets 1a&1b: Fruits

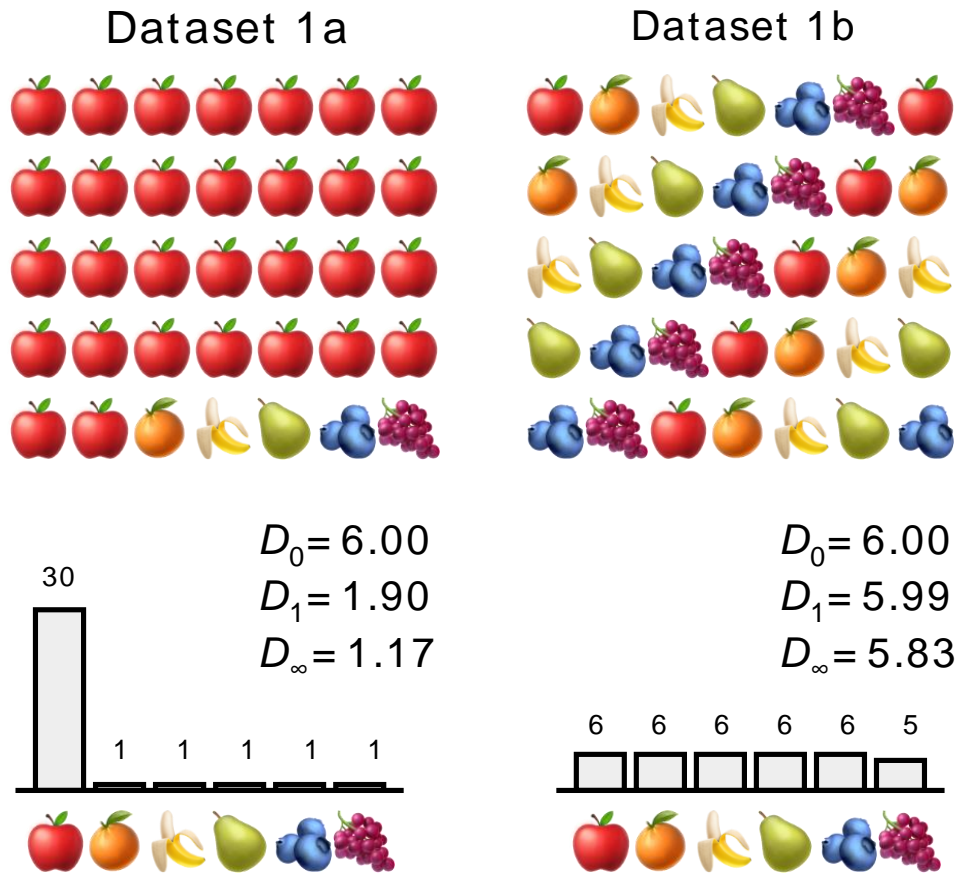
Dataset 1a	Dataset 1a	Dataset 1b
apple	30	6
orange	1	6
banana	1	6
pear	1	6
blueberry	1	6
grape	1	5
total	35	35

Table 3: *greylock* output for Dataset 1a

	community	viewpoint	alpha	rho	beta	gamma	normalized_ alpha	normalized_r ho	normalized_ beta
0	metacommu nity	0.00	6.00	1.00	1.00	6.00	6.00	1.00	1.00
1	Community 1	0.00	6.00	1.00	1.00	6.00	6.00	1.00	1.00
2	metacommu nity	1.00	1.90	1.00	1.00	1.90	1.90	1.00	1.00
3	Community 1	1.00	1.90	1.00	1.00	1.90	1.90	1.00	1.00
4	metacommu nity	inf	1.17	1.00	1.00	1.17	1.17	1.00	1.00
5	Community 1	inf	1.17	1.00	1.00	1.17	1.17	1.00	1.00

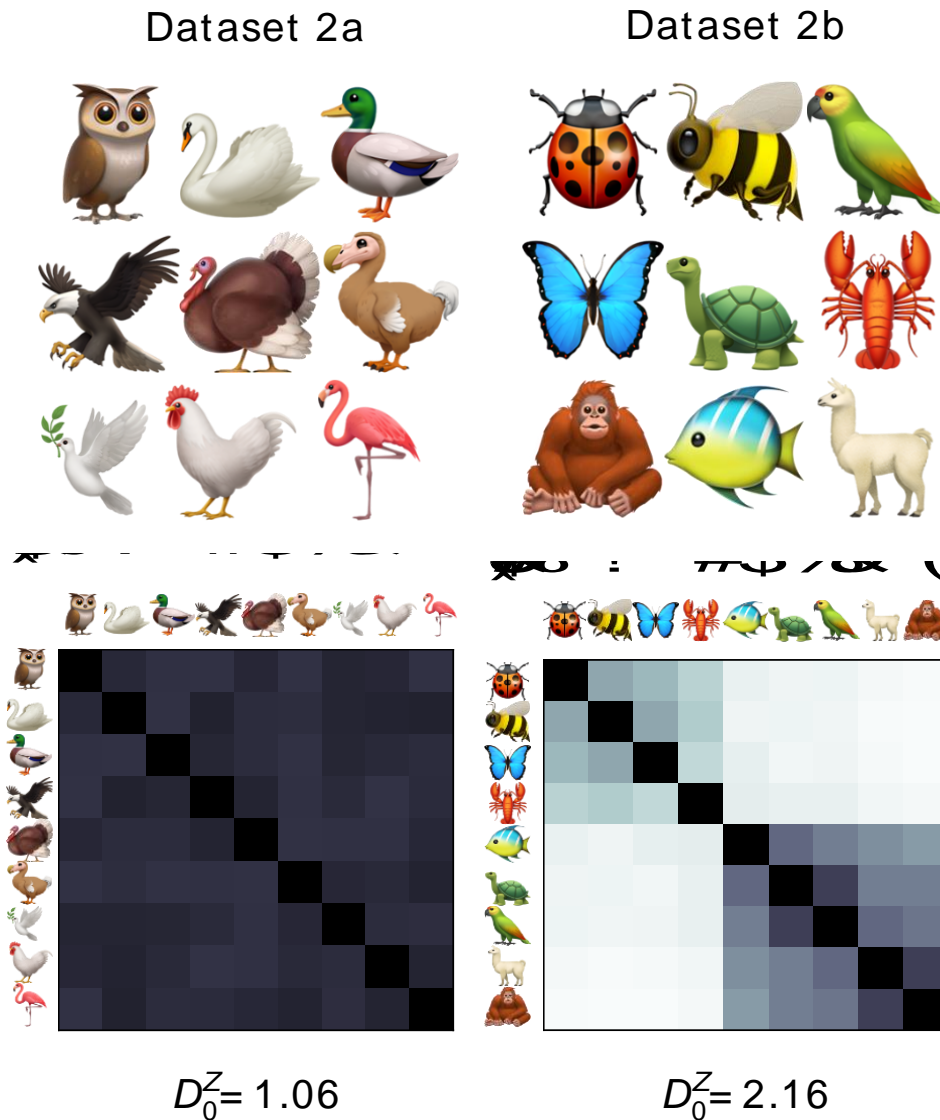
Note that with just a single community, the metacommunity and the community are the same. The apparently duplicate rows are output for consistency with situations where they are not the same.

Fig. 1: How frequency affects diversity



Each dataset contains six unique elements, so $D_0 = 6$ for each dataset (the “0” in D_0 makes D_0 frequency *insensitive*). Thus, if we ignore frequency, the two datasets are equally diverse. However, Dataset 1a is mostly apples, while Dataset 1b has a nearly uniform distribution of different fruits. Thus, Dataset 1b is intuitively more diverse. Consistent with intuition, D_1 is only 1.9 for Dataset 1a but nearly 6 for Dataset 2: for $q = 1$, Dataset 1a *effectively* has only 1.9 unique elements: one can think of this as the apple counting as one unique element and the other fruits in Dataset 1a collectively counting as nearly (0.9) the equivalent of a second unique element. Up-weighting common elements can also be thought of as discounting rare ones; thus, different values of q can be thought of as different discount factors, and therefore lead to different effective numbers. For example, for $q = \infty$, $D_\infty = 1.17$ for Dataset 1a and 5.83 for Dataset 2: with maximal discounting, Dataset 1a effectively has only fractionally more than a single element (effectively nearly all apples), whereas Dataset 1b still has close to all six (with a slight discount because there are only five bunches of grapes vs. six of each of the other fruits). The *greylock* package can calculate any frequency-sensitive diversity measure.

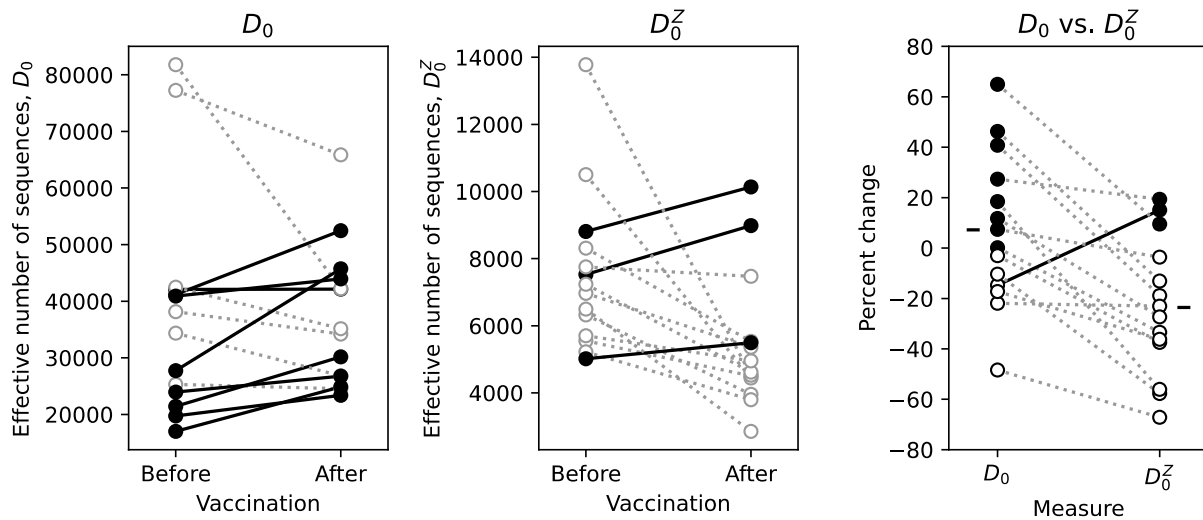
Fig. 2: How similarity affects diversity



Each dataset contains nine species (top), each at equal frequencies, so $D_0 = D_1 = D_2 = \dots = D_\infty = 9$ for each dataset. Thus, the two datasets are equally diverse using similarity-insensitive measures. However, Dataset 2a is all birds, whereas Dataset 2b contains a wider variety of animals, making Dataset 2b intuitively more diverse. The similarity matrices Z are accordingly quite different (bottom). Consistent with the intuition, D_0^Z is only 1.06 for Dataset 2a, but 2.16 for Dataset 2b: Dataset 2a effectively has only 1.06 species (further interpreted as it contains just a single class or type—here, birds; the “extra” 0.06 reflects intragroup diversity among bird species). Meanwhile, Dataset 2b effectively has 2.16 species, corresponding roughly to the number of taxonomic phyla represented (Arthropoda and Chordata, which form two visible

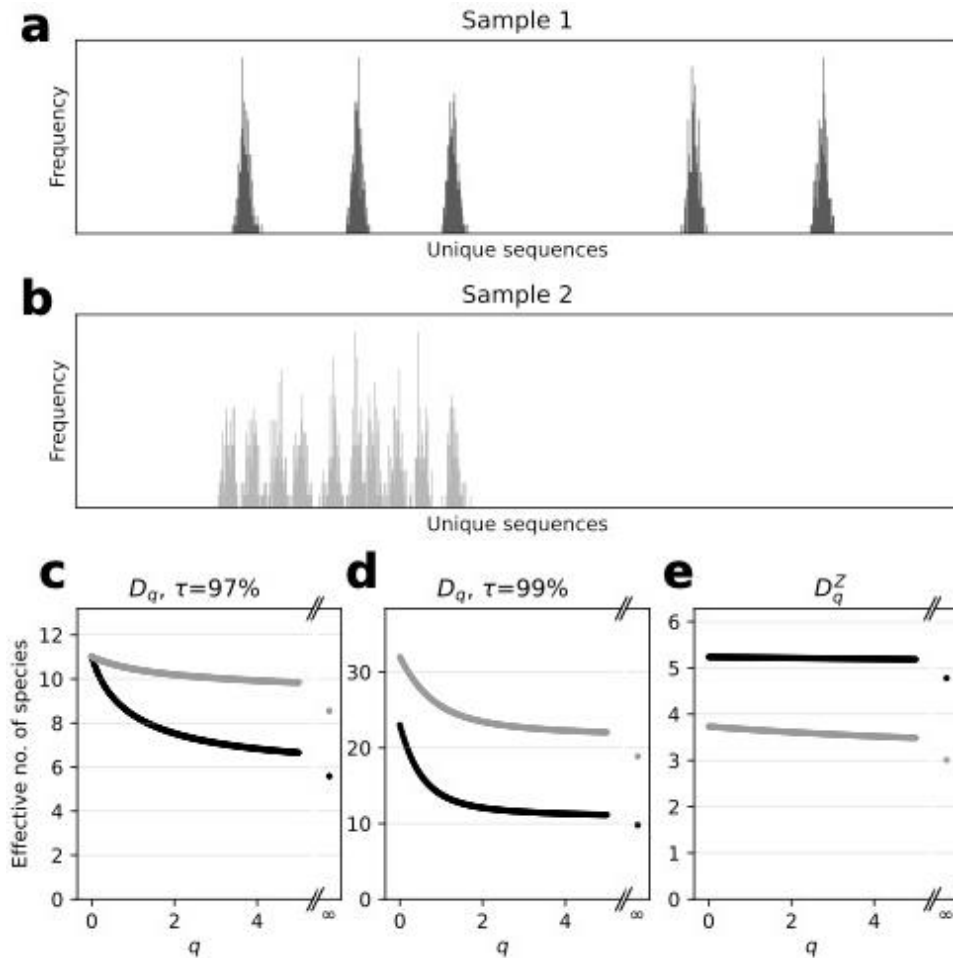
clusters in the similarity matrix). The *greylock* package can calculate any similarity-sensitive diversity measure for any user-supplied definition of similarity.

Fig 3: Immunomics: Similarity-insensitive vs. -sensitive measures in influenza vaccination



Diversity of IGH CDR3 immunomes according to the similarity-insensitive measure D_0 (left) and its similarity-sensitive counterpart D_0^Z (middle), and a comparison of the two (right) before vs. after influenza vaccination. Left and middle: light/dotted lines denote subjects where diversity falls. Right: each line/pair of symbols show D_0 and D_0^Z for the same subject. Dark line shows the one subject where vaccination was associated with fewer, more different sequences. Dashes in the margins indicate averages of D_0 and D_0^Z .

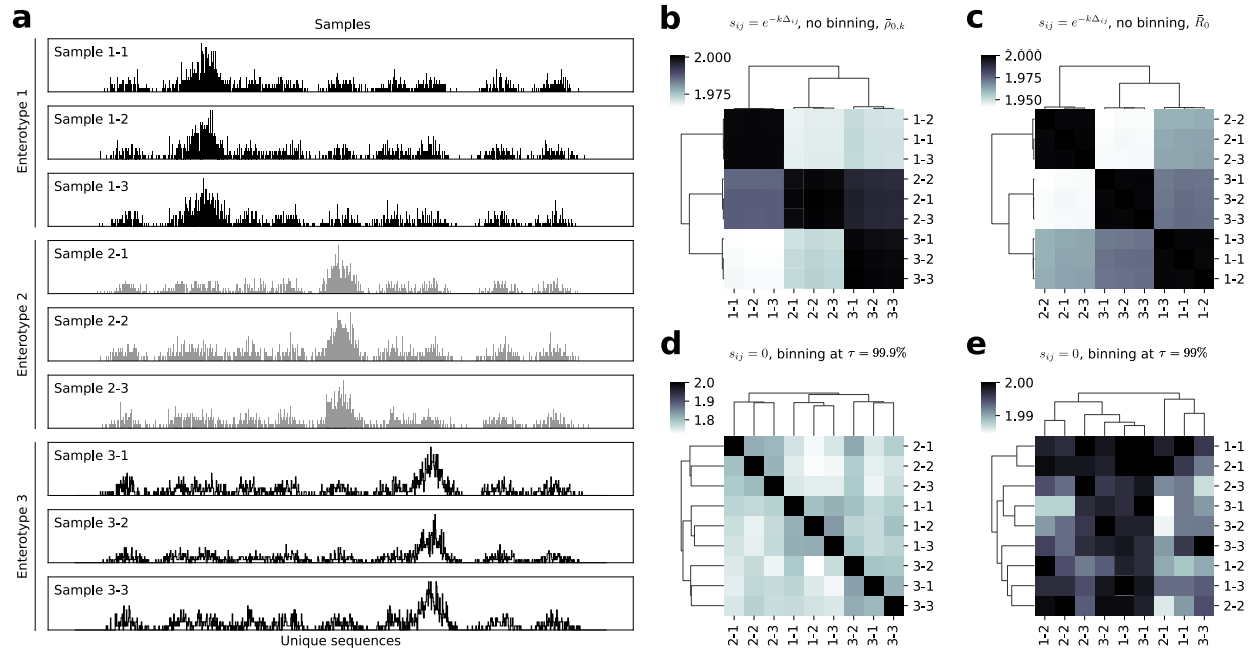
Fig. 4: Metagenomics: Similarity-insensitive vs. -sensitive alpha diversities in synthetic samples



Sample 1 (a) and 2 (b) both have 1,000 sequences. For ease of illustration, distance along the x-axis is proportional to similarity (i.e. more similar sequences are nearer each other). In Sample 1, sequences form five highly distinct clusters. In Sample 2, sequences form 10 more similar clusters. The distribution of sequences within each cluster is Gaussian, consistent with observations from the Human Microbiome Project [11]. Using binning to account for similarity and then measuring diversity using similarity-insensitive measures (D_q), diversity depends on the binning threshold τ and frequency weighting q . (c) At $\tau = 97\%$ and $q = 0$, the two samples are equally diverse, with $D_0 = 11$ species; At higher q , Sample 2 is more diverse, with diversities falling to $D_\infty = 8.6$ vs. $D_\infty = 5.6$ species, respectively, at $q = \infty$. (d) At $\tau = 99\%$, both samples are much more diverse, with $D_0 = 32$ vs. $D_0 = 23$ species, respectively. (Note that at this τ , Sample 2 is more diverse than Sample 1 for all q .) (e) In contrast, accounting for similarity using similarity-sensitive diversity measures (D_q^Z), which avoids the need for binning, the order flips: Sample 1 is

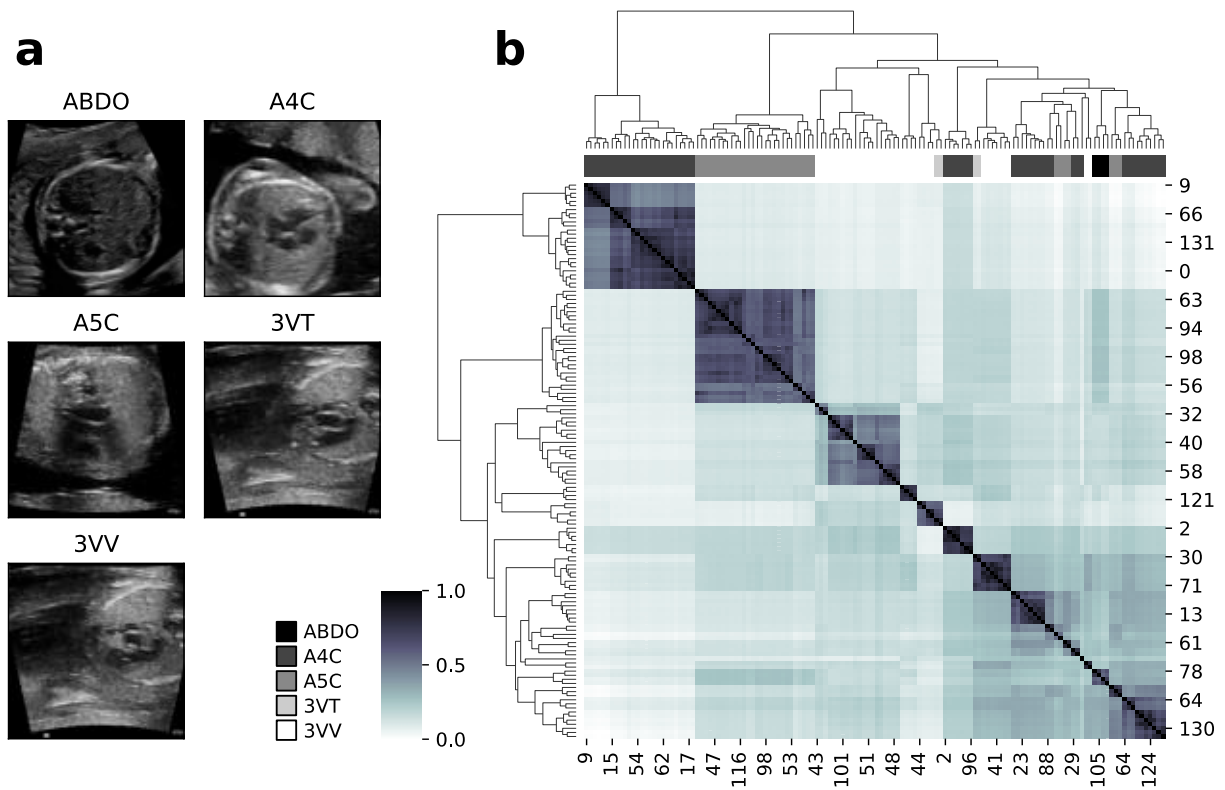
now more diverse than Sample 2 (for all q), with ~ 5 vs. $\sim 3-4$ species, respectively, reflecting both the number and the grouping of the clusters. (Here similarity s_{ij} between sequences i and j is calculated as $s_{ij} = e^{-k\Delta_{ij}}$, where Δ_{ij} is the Levenshtein distance between sequences i and j and $k = 0.02$.)

Fig. 5: Metagenomics: Beta diversities to elucidate population structure in synthetic samples



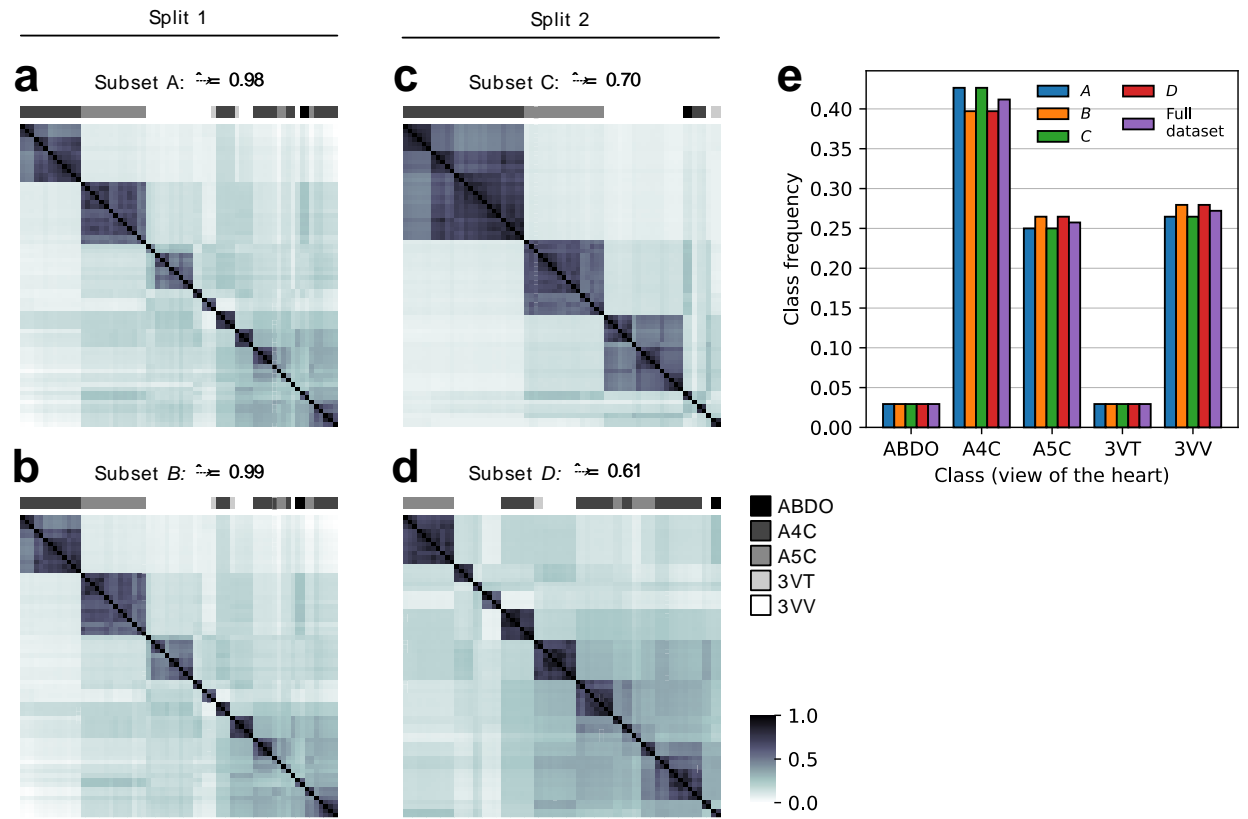
(a) Nine synthetic samples created as in Fig. 4a-b, three representing each of three enterotypes: black, Enterotype 1 (Samples 1-1 to 1-3); gray, Enterotype 2 (Samples 2-1 to 2-3); white, Enterotype 3 (Samples 3-1 to 3-3). (b)-(c) Clustering using similarity s_{ij} between sequences i and j as defined in Fig. 4 without binning, according to (b) the $q = 0$ representativeness ($\bar{\rho}_0$) of the k^{th} sample for the pair of samples indicated by the heatmap cell and (c) the average representativeness of each member of the pair (\bar{R}_0).

Fig 6. Medical imaging: Dataset structure



Example images from each labeled class (a) and heatmap of the similarity matrix for all 136 images (b) with several clusters of similar images clearly visible along the diagonal, often but not always correlating with the class label. The bar above the heatmap indicates the view (class label) of each image (ABDO, A4C, A5C, 3VT, 3VV). Similarity here is based on root-mean-square error (RMSE) of pixel differences between images i and j according to $s_{ij} = e^{-\text{RMSE}_{ij}}$. Identical images have a similarity of 1 and completely distinct images have a similarity approaching 0. Note that while RMSE is not invariant to rotation or translation, ultrasound images (like many medical images) have a privileged orientation and position.

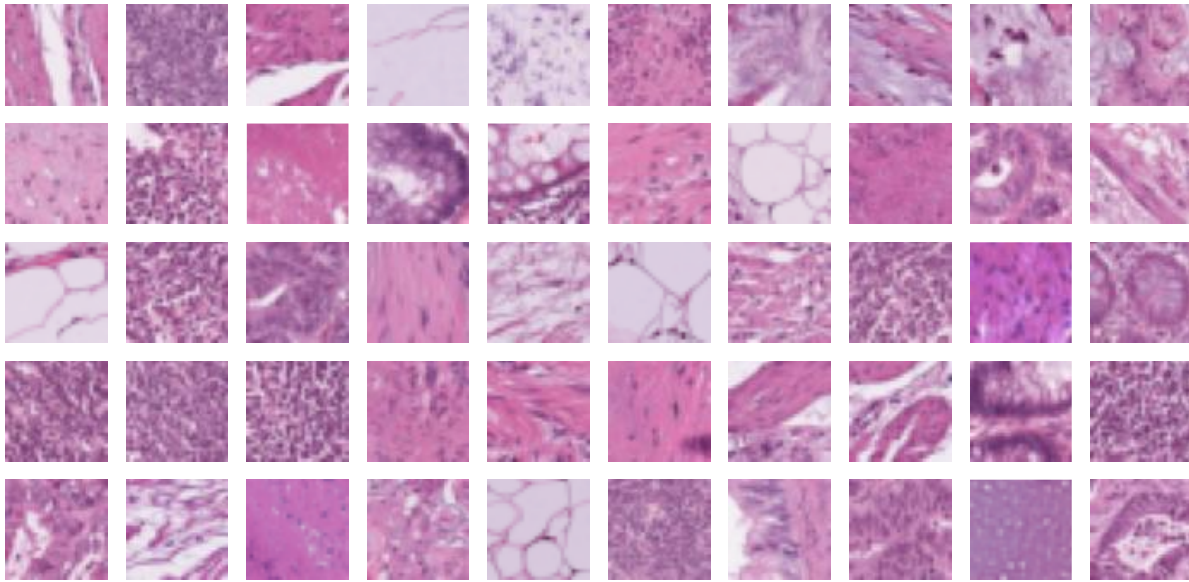
Fig. 7: Medical imaging: Representative and non-representative dataset splits



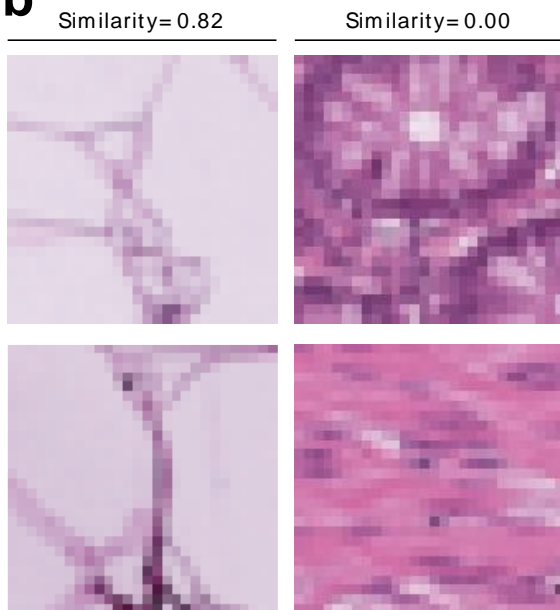
Heatmaps of similarity matrices for subsets of the dataset in Fig. 6. The dataset was split in half into subsets *A* (a) and *B* (b), and separately into subsets *C* (c) and *D* (d). Although all subsets were identically sized and indistinguishable in terms of class balance (e), $\hat{\rho}_k$ indicates that *A* and *B* are redundant while *C* and *D* are complementary.

Fig. 8: Computational pathology: Capturing dataset diversity in random subsets

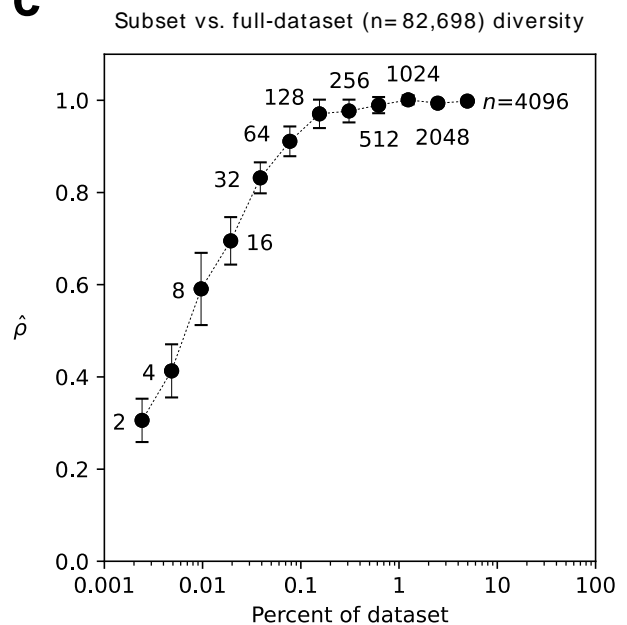
a



b



c



(a) Representative selection of images in the PathMNIST training set. (b) Pairs of high-similarity (left) and low-similarity (right) images according to an expert-defined similarity function. For comparison, two human subject-matter experts rated the similarity of the left pair as 0.8 and 0.9, and the right pair 0.0 and 0.0. (c) $\hat{\rho}$ for random subsets of images from the dataset. The x-axis indicates what percent of the full dataset each subset is; number of images is listed next to each datapoint. Error bars are s.d. for 10 independent random samples. Diagonal is the 1:1 line.

Dotted line is a guide to the eye. The inflection point at 128 images indicates diminishing returns.

References

- [1] M. O. Hill, "Diversity and Evenness: A Unifying Notation and Its Consequences," *Ecology*, vol. 54, no. 2, Art. no. 2, 1973, doi: 10.2307/1934352.
- [2] T. Leinster and C. A. Cobbold, "Measuring diversity: the importance of species similarity," *Ecology*, vol. 93, no. 3, Art. no. 3, Mar. 2012.
- [3] L. Jost, "Entropy and diversity," *Oikos*, vol. 113, no. 2, Art. no. 2, 2006, doi: 10.1111/j.2006.0030-1299.14714.x.
- [4] W. H. Berger and F. L. Parker, "Diversity of planktonic foraminifera in deep-sea sediments," *Science*, vol. 168, no. 3937, Art. no. 3937, Jun. 1970, doi: 10.1126/science.168.3937.1345.
- [5] L. Jost, "PARTITIONING DIVERSITY INTO INDEPENDENT ALPHA AND BETA COMPONENTS," *Ecology*, vol. 88, no. 10, pp. 2427–2439, Oct. 2007, doi: 10.1890/06-1736.1.
- [6] L. Jost, "What do we mean by diversity? The path towards quantification," *Métode*, no. 9, Jul. 2018, doi: 10.7203/metode.9.11472.
- [7] T. Leinster, "Entropy and Diversity: The Axiomatic Approach," *arXiv preprint arXiv:2012.02113*, 2020.
- [8] Z. Wang, A. C. Bovik, H. R. Sheikh, and E. P. Simoncelli, "Image quality assessment: from error visibility to structural similarity," *IEEE transactions on image processing*, vol. 13, no. 4, pp. 600–612, 2004.
- [9] E. Chinn, R. Arora, R. Arnaout, and R. Arnaout, "ENRICHing medical imaging training sets enables more efficient machine learning," *Journal of the American Medical Informatics Association*, vol. 30, no. 6, pp. 1079–1090, Jun. 2023, doi: 10.1093/jamia/ocad055.
- [10] R. Arora and R. Arnaout, "Repertoire-scale measures of antigen binding," *Proc. Natl. Acad. Sci. U.S.A.*, vol. 119, no. 34, p. e2203505119, Aug. 2022, doi: 10.1073/pnas.2203505119.

- [11] N.-P. Nguyen, T. Warnow, M. Pop, and B. White, "A perspective on 16S rRNA operational taxonomic unit clustering using sequence similarity," *npj Biofilms Microbiomes*, vol. 2, no. 1, p. 16004, Nov. 2016, doi: 10.1038/npjbiofilms.2016.4.
- [12] R. C. Edgar, "Updating the 97% identity threshold for 16S ribosomal RNA OTUs," *Bioinformatics*, vol. 34, no. 14, pp. 2371–2375, Jul. 2018, doi: 10.1093/bioinformatics/bty113.
- [13] J. Kaplinsky, A. Li, A. Sun, M. Coffre, S. B. Koralov, and R. Arnaout, "Antibody repertoire deep sequencing reveals antigen-independent selection in maturing B cells," *Proc Natl Acad Sci U S A*, vol. 111, no. 25, Art. no. 25, Jun. 2014, doi: 10.1073/pnas.1403278111.
- [14] J. Couch *et al.*, "Scaling Monte-Carlo-Based Inference on Antibody and TCR Repertoires." arXiv, Dec. 19, 2023. doi: 10.48550/arXiv.2312.12525.
- [15] R. Reeve *et al.*, "How to partition diversity," *arXiv:1404.6520 [q-bio]*, Apr. 2014, Accessed: Sep. 18, 2019. [Online]. Available: <http://arxiv.org/abs/1404.6520>
- [16] J. Kaplinsky and R. Arnaout, "Robust estimates of overall immune-repertoire diversity from high-throughput measurements on samples," *Nat Commun*, vol. 7, no. 1, p. 11881, Sep. 2016, doi: 10.1038/ncomms11881.
- [17] C.-H. Chiu and A. Chao, "Distance-Based Functional Diversity Measures and Their Decomposition: A Framework Based on Hill Numbers," *PLOS ONE*, vol. 9, no. 7, Art. no. 7, Jul. 2014, doi: 10.1371/journal.pone.0100014.
- [18] R. Reeve and C. Harris, "Diversity.jl - diversity measurement in Julia." 2019. [Online]. Available: <https://github.com/EcoJulia/Diversity.jl>
- [19] S. Mitchell, R. Reeve, and T. White, "rdiversity - Measurement and Partitioning of Similarity-Sensitive Biodiversity." 2022. [Online]. Available: <https://github.com/boydorr/rdiversity>
- [20] R. A. Arnaout, E. T. L. Prak, N. Schwab, F. Rubelt, and the Adaptive Immune Receptor Repertoire Community, "The Future of Blood Testing Is the Immunome," *Front. Immunol.*, vol. 12, p. 626793, Mar. 2021, doi: 10.3389/fimmu.2021.626793.
- [21] A. Pelissier, "cdiversity: Quantifying B-Cell Clonal Diversity In Repertoire Data." Accessed: Dec. 21, 2023. [Online]. Available: <https://github.com/Aurelien-Pelissier/cdiversity>

- [22] A. Pelissier, S. Luo, M. Stratigopoulou, J. E. J. Guikema, and M. Rodríguez Martínez, "Exploring the impact of clonal definition on B-cell diversity: implications for the analysis of immune repertoires," *Front Immunol*, vol. 14, p. 1123968, 2023, doi: 10.3389/fimmu.2023.1123968.
- [23] R. Arnaout *et al.*, "High-resolution description of antibody heavy-chain repertoires in humans," *PLoS One*, vol. 6, no. 8, Art. no. 8, 2011, doi: 10.1371/journal.pone.0022365.
- [24] B. Briney, A. Inderbitzin, C. Joyce, and D. R. Burton, "Commonality despite exceptional diversity in the baseline human antibody repertoire," *Nature*, vol. 566, no. 7744, Art. no. 7744, Feb. 2019, doi: 10.1038/s41586-019-0879-y.
- [25] C. Soto *et al.*, "High frequency of shared clonotypes in human B cell receptor repertoires," *Nature*, vol. 566, no. 7744, Art. no. 7744, Feb. 2019, doi: 10.1038/s41586-019-0934-8.
- [26] J. Chiffelle, R. Genolet, M. A. Perez, G. Coukos, V. Zoete, and A. Harari, "T-cell repertoire analysis and metrics of diversity and clonality," *Current Opinion in Biotechnology*, vol. 65, pp. 284–295, Oct. 2020, doi: 10.1016/j.copbio.2020.07.010.
- [27] C. Vollmers, R. V. Sit, J. A. Weinstein, C. L. Dekker, and S. R. Quake, "Genetic measurement of memory B-cell recall using antibody repertoire sequencing," *Proc. Natl. Acad. Sci. U.S.A.*, vol. 110, no. 33, Art. no. 33, Aug. 2013, doi: 10.1073/pnas.1312146110.
- [28] J. S. Johnson *et al.*, "Evaluation of 16S rRNA gene sequencing for species and strain-level microbiome analysis," *Nat Commun*, vol. 10, no. 1, p. 5029, Dec. 2019, doi: 10.1038/s41467-019-13036-1.
- [29] C. Lozupone and R. Knight, "UniFrac: a New Phylogenetic Method for Comparing Microbial Communities," *Appl Environ Microbiol*, vol. 71, no. 12, pp. 8228–8235, Dec. 2005, doi: 10.1128/AEM.71.12.8228-8235.2005.
- [30] M. Arumugam *et al.*, "Enterotypes of the human gut microbiome," *Nature*, vol. 473, no. 7346, pp. 174–180, May 2011, doi: 10.1038/nature09944.
- [31] C. A. Lozupone, J. I. Stombaugh, J. I. Gordon, J. K. Jansson, and R. Knight, "Diversity, stability and resilience of the human gut microbiota," *Nature*, vol. 489, no. 7415, pp. 220–230, Sep. 2012, doi: 10.1038/nature11550.

- [32] L. M. Petersen *et al.*, “Community characteristics of the gut microbiomes of competitive cyclists,” *Microbiome*, vol. 5, no. 1, pp. 1–13, 2017.
- [33] M. Cheng and K. Ning, “Stereotypes About Enterotype: the Old and New Ideas,” *Genomics Proteomics Bioinformatics*, vol. 17, no. 1, pp. 4–12, Feb. 2019, doi: 10.1016/j.gpb.2018.02.004.
- [34] X. Zhou *et al.*, “Exploratory studies of oral and fecal microbiome in healthy human aging,” *Front Aging*, vol. 3, p. 1002405, 2022, doi: 10.3389/fragi.2022.1002405.
- [35] G. D. Wu *et al.*, “Linking long-term dietary patterns with gut microbial enterotypes,” *Science*, vol. 334, no. 6052, pp. 105–108, Oct. 2011, doi: 10.1126/science.1208344.
- [36] R. Arnaout, L. Curran, Y. Zhao, J. C. Levine, E. Chinn, and A. J. Moon-Grady, “An ensemble of neural networks provides expert-level prenatal detection of complex congenital heart disease,” *Nat Med*, vol. 27, no. 5, Art. no. 5, May 2021, doi: 10.1038/s41591-021-01342-5.
- [37] A. E. Kornblith *et al.*, “Development and Validation of a Deep Learning Strategy for Automated View Classification of Pediatric Focused Assessment With Sonography for Trauma,” *J Ultrasound Med*, vol. 41, no. 8, pp. 1915–1924, Aug. 2022, doi: 10.1002/jum.15868.
- [38] C. Athalye, A. van Nesselrooij, S. Rizvi, M. Haak, A. J. Moon-Grady, and R. Arnaout, “Deep learning model for prenatal congenital heart disease (CHD) screening can be applied to retrospective imaging from the community setting, outperforming initial clinical detection in a well-annotated cohort,” *Ultrasound Obstet Gynecol*, Sep. 2023, doi: 10.1002/uog.27503.
- [39] D. L. Ferreira, Z. Salaymang, and R. Arnaout, “Label-free segmentation from cardiac ultrasound using self-supervised learning,” *ArXiv*, vol. abs/2210.04979, 2022, [Online]. Available: <https://api.semanticscholar.org/CorpusID:252815884>
- [40] C. Athalye and R. Arnaout, “Domain-guided data augmentation for deep learning on medical imaging,” *PLoS One*, vol. 18, no. 3, p. e0282532, 2023, doi: 10.1371/journal.pone.0282532.
- [41] J. Yang *et al.*, “MedMNIST v2 - A large-scale lightweight benchmark for 2D and 3D biomedical image classification,” *Scientific Data*, vol. 10, no. 1, p. 41, Jan. 2023, doi: 10.1038/s41597-022-01721-8.

- [42] D. Dey *et al.*, “Proceedings of the NHLBI Workshop on Artificial Intelligence in Cardiovascular Imaging: Translation to Patient Care.,” *JACC Cardiovasc Imaging*, vol. 16, no. 9, pp. 1209–1223, Sep. 2023, doi: 10.1016/j.jcmg.2023.05.012.

Supplementary Material

Availability and installation

The *greylock* package is available on GitHub at <https://github.com/ArnaoutLab/diversity>. It can be installed by running

```
pip install greylock
```

from the command-line interface. The test suite runs successfully on Macintosh, Windows, and Unix systems. The unit tests and coverage report can also be run by

```
pytest --pyargs greylock --cov greylock
```

Basic usage: alpha diversities

We illustrate the basic usage of *greylock* on simple datasets of fruits (Fig. 1) and animals (Fig. 2) because these are discipline agnostic and easy to interpret. To better connect to previous work [7], we will use the term “subcommunity” synonymously with “dataset” and the term “metacommunity” whenever datasets are combined. (Note, when there is only a single dataset under study, the subcommunity *is* the metacommunity.)

First, consider two datasets, each with 35 total elements. Each dataset has the same $n = 6$ unique elements, each a type of fruit: apples, oranges, bananas, pears, blueberries, and grapes (Fig. 1). Dataset 1a is mostly apples; in dataset 1b, all fruits are represented at almost identical frequencies (Table 2).

We wish to apply *greylock* to these datasets, being sensitive to the essential difference between the two: the difference in frequencies of the unique elements. To do so, we first specify a species counts table, formatted as in Table 2.

A frequency-sensitive metacommunity can be created in Python by passing a counts DataFrame to a `Metacommunity` object:

```
import pandas as pd
import numpy as np
from greylock import Metacommunity
counts_1a = pd.DataFrame({"Dataset 1a": [30, 1, 1, 1, 1, 1]}, index=["apple",
"orange", "banana", "pear", "blueberry", "grape"])
```

```
metacommunity_1a = Metacommunity(counts_1a)
```

Now that the metacommunity has been created, diversity measures can be calculated. For example, to calculate D_1 , we type:

```
metacommunity_1a.subcommunity_diversity(viewpoint=1, measure='alpha')
```

which yields the output:

```
array([1.89654919])
```

The output shows that $D_1 = 1.8965 \dots \approx 1.90$. To calculate multiple diversity measures at once and store them in a DataFrame, we type:

```
metacommunity_1a.to_dataframe(viewpoint=[0, 1, np.inf])
```

which produces the output in Table 3.

Similarly, we find that $D_1 \approx 5.99$ for Dataset 1b (Fig. 1). The larger value of D_1 for Dataset 1b aligns with the intuitive sense that more balance in the frequencies of unique elements means a more diverse dataset.

greylock can also calculate similarity-sensitive diversity measures for any user-supplied definition of similarity. To illustrate, we now consider a second example in which the dataset elements are all unique. Uniqueness means element frequencies are identical, so similarity is the only factor that can influence our sense of whether one or the other dataset is more diverse. The datasets in Fig. 2 each contain a set of animals in which each animal appears only once. The investigator always has a choice of similarity measure, which they can choose to investigate the question at hand; here we consider (approximate) phylogenetic similarity. Dataset 2a consists entirely of birds, so all entries in the similarity matrix are close to 1:

```
labels_2a = ["owl", "eagle", "flamingo", "swan", "duck", "chicken", "turkey",  
            "dodo", "dove"]  
no_species_2a = len(labels_2a)  
S_2a = np.identity(n=no_species_2a)  
S_2a[0][1:9] = (0.91, 0.88, 0.88, 0.88, 0.88, 0.88, 0.88, 0.88) # owl  
S_2a[1][2:9] = ( 0.88, 0.89, 0.88, 0.88, 0.88, 0.88, 0.89, 0.88) # eagle  
S_2a[2][3:9] = ( 0.90, 0.89, 0.88, 0.88, 0.88, 0.88, 0.89) # flamingo
```

```

S_2a[3][4:9] = (          0.92, 0.90, 0.89, 0.88, 0.88) # swan
S_2a[4][5:9] = (          0.91, 0.89, 0.88, 0.88) # duck
S_2a[5][6:9] = (          0.92, 0.88, 0.88) # chicken
S_2a[6][7:9] = (          0.89, 0.88) # turkey
S_2a[7][8:9] = (          0.88) # dodo
                                     # dove

S_2a = np.maximum( S_2a, S_2a.transpose() )
S_2a = pd.DataFrame({labels_2a[i]: S_2a[i] for i in range(no_species_2a)},
                    index=labels_2a)

```

We make a DataFrame of counts in the same way as in the previous example:

```

counts_2a = pd.DataFrame({"Community 2a": [1, 1, 1, 1, 1, 1, 1, 1, 1, 1]},
                        index=labels_2a)

```

To compute similarity-sensitive diversity measures, we now pass the similarity matrix as the similarity argument of the metacommunity object:

```

metacommunity_2a = Metacommunity(counts_2a, similarity=S_2a)

```

We can find D_1^Z (using $q = 1$ just for comparison to the previous example) similarly to the above:

```

metacommunity_2a.subcommunity_diversity(viewpoint=1, measure='alpha')

```

This produces the output:

```

array([1.09908705])

```

The output tells us that $D_1^Z \approx 1.10$. The fact that this number is close to 1 reflects the fact that all individuals in this community are phylogenetically very similar to each other: they are all birds.

In contrast, Dataset 2b (Fig. 2) consists of members from two different phyla: vertebrates and invertebrates. As above, we define a similarity matrix:

```

labels_2b = ("ladybug", "bee", "butterfly", "lobster", "fish", "turtle",
            "parrot", "llama", "orangutan")
no_species_2b = len(labels_2b)
S_2b = np.identity(n=no_species_2b)
S_2b[0][1:9] = (0.60, 0.55, 0.45, 0.25, 0.22, 0.23, 0.18, 0.16) # ladybug
S_2b[1][2:9] = ( 0.60, 0.48, 0.22, 0.23, 0.21, 0.16, 0.14) # bee

```

```

S_2b[2][3:9] = (          0.42, 0.27, 0.20, 0.22, 0.17, 0.15) # butterfly
S_2b[3][4:9] = (          0.28, 0.26, 0.26, 0.20, 0.18) # lobster
S_2b[4][5:9] = (          0.75, 0.70, 0.66, 0.63) # fish
S_2b[5][6:9] = (          0.85, 0.70, 0.70) # turtle
S_2b[6][7:9] = (          0.75, 0.72) # parrot
S_2b[7][8:9] = (          0.85) # llama
                                     #orangutan

S_2b = np.maximum( S_2b, S_2b.transpose() )
S_2b = pd.DataFrame({labels_2b[i]: S_2b[i] for i in range(no_species_2b)},
index=labels_2b)

```

The values of the similarity matrix indicate high similarity among the vertebrates, high similarity among the invertebrates, and low similarity between vertebrates and invertebrates.

To calculate the alpha diversity (with $q = 1$ as above), we proceed as before, defining counts, creating a Metacommunity object, and calling its `subcommunity_diversity` method with the desired settings:

```

counts_2b = pd.DataFrame({"Community 2b": [1, 1, 1, 1, 1, 1, 1, 1, 1, 1]},
index=labels_2b)
metacommunity_2b = Metacommunity(counts_2b, similarity=S_2b)
metacommunity_2b.subcommunity_diversity(viewpoint=1, measure='alpha')

```

This outputs:

```
array([2.14151583])
```

Thus, $D_1^Z \approx 2.14$. That this number is close to 2 reflects the fact that members in this community belong to two broad classes of animals: vertebrates and invertebrates. The remaining 0.14 above 2 is interpreted as the contribution of the diversity within each phylum. Note that if we had instead simply placed animals into two bins, vertebrates and invertebrates, this contribution would be lost.

Basic usage: beta diversities

Recall that beta diversity is between-group diversity. We can use *greylock* to compare the diversity of the vertebrates and invertebrates. To do so, we re-imagine Dataset 2b as a

metacommunity made up of 2 subcommunities—the invertebrates and the vertebrates—defined as follows:

```
counts_2b_1 = pd.DataFrame(  
{  
    "Subcommunity_2b_1": [1, 1, 1, 1, 0, 0, 0, 0, 0], # invertebrates  
    "Subcommunity_2b_2": [0, 0, 0, 0, 1, 1, 1, 1, 1], # vertebrates  
},  
index=labels_2b  
)
```

We then obtain the representativeness $\hat{\rho}$ of each subcommunity, here at $q = 0$, as follows:

```
metacommunity_2b_1 = Metacommunity(counts_2b_1, similarity=S_2b)  
metacommunity_2b_1.subcommunity_diversity(viewpoint=0,  
measure='rho_hat')
```

This outputs:

```
array([0.41333318, 0.21398288])
```

Recall $\hat{\rho}$ indicates how well a subcommunity represents the metacommunity. We find that $\hat{\rho}$ of the two subcommunities are rather low—0.41 and 0.21 for the invertebrates and the vertebrates, respectively—reflecting the low similarity between these groups.

Note we can also ask which subset is more diverse by calculating the alpha diversities of the two subcommunities (also at $q = 0$, for ease of comparison):

```
Metacommunity_2b_1.subcommunity_diversity(viewpoint=0, measure='alpha')
```

This outputs:

```
array([3.53787004, 2.29512853])
```

We find that the invertebrates ($D_2^q \approx 3.54$) are more diverse than the vertebrates ($D_2^q \approx 2.30$).

In contrast, suppose we split Dataset 2b into two subsets at random, without regard to phylum:

```
counts_2b_2 = pd.DataFrame(  
{
```



```

    "Subcommunity_2b_3": [1, 0, 1, 0, 1, 0, 1, 0, 1],
    "Subcommunity_2b_4": [0, 1, 0, 1, 0, 1, 0, 1, 0],
},
index=labels_2b
)

```

Proceeding again as above:

```

metacommunity_2b_2 = Metacommunity(counts_2b_2, similarity=S_2b)
metacommunity_2b_2.subcommunity_diversity(viewpoint=0, measure='rho_hat')

```

This yields:

```
array([0.67824819, 1.06877778])
```

we find that the $\hat{\rho}$ of the two subsets are now, respectively, 0.68 and 1.07. These high values reflect the fact that each group now has a roughly equal mix of vertebrates and invertebrates.

Advanced usage: similarity matrix format

The similarity matrix format—`DataFrame`, `memmap`, `filepath`, or `function`—should be chosen based on the use case, with particular attention to dataset size. Our recommendations:

- If the similarity matrix fits in RAM, pass it as a `pandas.DataFrame` or `numpy.ndarray`
- If the similarity matrix does not fit in RAM but does fit on your hard drive (HD), pass it as a `csv/tsv filepath` or `numpy.memmap`
- If the similarity matrix does not fit in either RAM or HD, pass a similarity function and the feature-set file that will be used to calculate similarities. Note that construction of the similarity matrix is an $\mathcal{O}(N^2)$ operation; if your similarity function is expensive, this calculation can take time for large datasets, even though *greylock* natively runs parallelized, utilizing all available processing cores.

Command-line usage

The *greylock* package can also be used from the command line as a module (via `python -m`). The example below re-uses `counts_2b_1` and `S_2b` from above, saved as `.csv` files (note `index=False`, since the `csv` files do not contain row labels):

```
counts_2b_1.to_csv("counts_2b_1.csv", index=False)
```

```
S_2b.to_csv("S_2b.csv", index=False)
```

Then from the command line:

```
python -m greylock -i counts_2b_1.csv -s S_2b.csv -v 0 1 inf.
```

The output is a table with all the diversity measures for $q = 0$, 1 , and ∞ . Note that while `.csv` or `.tsv` are acceptable as input, the output is always tab-delimited. The input filepath (`-i`) and the similarity matrix filepath (`-s`) can be URLs to data files hosted on the web. Also note that values of $q > 100$ are all calculated as $q = \infty$.

For further options, consult the help:

```
python -m greylock -h
```